Nano Communication Networks 19 (2019) 1–9

Contents lists available at ScienceDirect

Nano Communication Networks

journal homepage: www.elsevier.com/locate/nanocomnet

Sensorless Node Architecture for Events detection in Self-Powered Nanosensor Networks

Najm Hassan [a,*], Marios Mattheakis [b], Ming Ding [c]

[a] School of Computer Science and Engineering (CSE), University of New South Wales (UNSW), Sydney, NSW 2052, Australia
[b] John A. Paulson School of Engineering and Applied Sciences, Harvard University, Cambridge, MA 02138, USA
[c] Data 61, CSIRO, Eveleigh, NSW 2015, Australia

ARTICLE INFO

Article history:
Received 30 May 2018
Received in revised form 1 September 2018
Accepted 25 October 2018
Available online 10 November 2018

Keywords:
Surface plasmon polaritons
Graphene
Evanescent source
Near-field excitation
Plasmonic transmitter

ABSTRACT

Due to size, computational and power limitations an integrated nanosensor device needs to be redesigned with a limited number of components. A sensorless event detection node can overcome these limitations where such node can be powered using energy harvested from various events. The harvested energy could also be a significant factor for events detection without using any sensors. This study presents a detailed description of a sensorless event detection node which consists of two components — an energy harvester and a pulse generator. We discuss the state of the art configurations for these two components. However, due to the low complexity of the nanoscale device, the pulse generator should be kept simple. We, therefore, theoretically investigate different approaches for the pulse generator to generate Surface Plasmon Polaritons (SPPs) which reasonably resemble femtoseconds long pulses in graphene. Based on our analysis, we find that SPPs can be excited using a near-field excitation method for the THz band which is simple and can produce Electromagnetic (EM) radiation with a wide range of high wavenumber. Hence, the coupling condition can be easily satisfied and consequently, the SPP wave can be excited. However, such method excites SPPs locally, which requires improvement in practice. Thus we numerically investigate how operating frequency, the doping amount of graphene and the properties of the evanescent source affect the plasmon resonance of SPPs. We also studied different evanescent sources such as electric dipole, and hexapole, and find that the former provides better SPP resonance. We also observe that through fine-tuning of the chemical potential, frequency and source phase angle, higher amplitude SPPs can be excited on graphene surface in the THz band. The proposed model can be a good candidate for a low-complexity realization of a THz pulse generator in self-powered sensorless events detection node.

1. Introduction

The advancements in nanotechnology made it possible to fabricate nodes at the nanoscale. These nanonodes are made from novel materials which have unique physical, electrical and optical properties and can sense molecule level events in immediate surroundings [1]. Nanosensors have the capabilities to sense a range of information at the molecular level in concentrations as low as one part per billion [2] however, the sensing scope is limited to the close environment of nanosensors usually a few micrometers. To read the sensed information and measurements, nanocommunication will be a key enabler to transmit the cell-level data to a remote station. However, wireless communication at the nanoscale has not been successfully realized yet. There are key relevant developments in recent years that head to a future when such devices could become commodities.

Recent simulation studies confirm that these nodes may be able to communicate in the terahertz band [3,4] ushering new Internet of Things (IoT) capabilities for gathering knowledge at an unprecedented depth and scale. Researcher are now pursuing this new direction of IoT under the banner of Internet of Nano-Things (IoNT) [5] with nano-scale monitoring techniques explored for human body [1,6], plants [7], chemical processes [8], and so on. These nodes generate SPP waves in graphene which reasonably resemble femtoseconds long pulses and radiate them in free space [3,9,10].

With the emergence of IoNT, researchers propose new communication standards for nanoscale devices to communicate with each other in diverse applications. They propose channel modeling [2], novel information coding techniques [11,12], energy harvesting schemes [9] and novel network architectures [1,13,14]. Amongst all, pulse-based communication which is based on the transmission of a hundred femtoseconds long pulses is proposed in [10].

Due to the small form factor, these nodes are extremely power restricted. So they are required to self-power themselves without relying on batteries. They are expected to harvest energy

* Corresponding author.
E-mail address: nhassan@cse.unsw.edu.au (N. Hassan).

https://doi.org/10.1016/j.nancom.2018.10.005
1878-7789/

from the events in the ambient environment. However, due to severe volume restrictions, these nodes are expected to generate power between fW to a few pW which is insufficient to power all nano-components in nanosensors [15]. To address the problem of powering nanosensors, a schematic sensorless event detection architecture is recently proposed in [15] to monitor event types remotely. Such framework uses the energy signatures of monitored events to efficiently detect events at the remote station. However, this work only focuses to model and design a sensorless event detection node in COMSOL Multiphysics which is close to the physical reality. We first provide a theoretical background of the sensorless node where we investigate state of the art configurations for energy harvesting and terahertz (THz) signal generator. We then proceed to investigate a simple architecture of signal generator within the sensorless node, in COMSOL Multiphysics, to generate the pulse in the THz band (THz). We expect that simple structures are more likely to succeed in the future design of nanodevices.

The pulse generator, which we will explain in Section 3, is used to generate the SPP wave (THz pulse) on the graphene surface. The SPP travels towards radio which radiates it in the free space. We show using COMSOL Multiphysics that SPP wave can be generated directly on graphene surface using the near-field method. This method excites SPPs locally and requires improvement in practice. Thus we explored how operating frequency, the doping amount of graphene and the properties of the evanescent source affect the plasmon resonance of SPPs.

Inspired from tip method in [16], where a laser irradiates a metallic tip with the radius much smaller than operation wavelength, we introduce a point source of nano dimension with radius $R = 20$ nm as a boundary condition for exciting SPPs on graphene sheet [17]. In this method, a TM polarized evanescent nanoscale source, such as a magnetic dipole or quadrupole, is located above graphene. This kind of sources with dimensions much smaller than the wavelength of EM radiation, produce EM radiation with very high wavenumbers k. Hence, the matching condition between k and k_{sp} is easily satisfied and consequently, SPP waves can be directly excited. It is important to note that SPP excitation using a femtosecond laser pulse is already proposed for wireless communications among nanosystems [18,19]. However, current work is different from the previous works in that it aims to generate SPP wave directly on graphene surface without employing specialized structure. The SPPs are excited locally and afterward, they propagate along the graphene surface. In practice, a nanoantenna converts these SPPs into propagating electromagnetic (EM) waves [3]. However, recent studies confirm that the enhancement of the antenna radiation is due to the resonance of surface plasmonic wave on graphene surface [20]. We, therefore, further aim to get high-quality SPP resonance on the graphene surface. To achieve this, we investigate different evanescent sources for SPPs excitation with phase shift and study the effect of each evanescent source on SPPs resonance. We observe that SPPs resonance on graphene shows a strong dependence on chemical doping as well as on the characteristics of the evanescent source, namely the type and the phase angle.

The key contributions of this paper are as follows:

- We present a detailed description of a sensorless event detection node in nanocommunication.
- In this numerical study, we investigate pulse generator within the event detection node using COMSOL Multiphysics. We model an excitation source in the THz band and notice that it can generate SPPs directly on the graphene surface.
- Briefly we discussed different configurations for excitation of SPP waves on metallic surfaces as well as on graphene. Specifically, for each method, we examined the coupling condition between incident EM waves and surface plasmons of metals, where this coupling leads to SPP formation.
- To achieve high amplitude SPP resonance, We optimize chemical doping as well as the characteristics of the excitation source, namely the type and the phase angle via numerical simulations. Thus, we find that through fine-tuning of the chemical potential, THz frequency, and source phase angle, higher amplitude SPPs can be excited on the graphene surface.

The rest of the paper is organized as follows: The fundamentals of SPP are reviewed in Section 2. In Section 3, we give detail of sensorless event detection node architecture. In Section 4, we present the proposed pulse generator which uses the near-field method to excite SPPs in the THz band. In Section 5 we provide the simulation results and discussion. Finally concluding remarks and future works are given in Section 6.

2. SPP preliminaries

Plasmon is the quantum state of plasma oscillation while surface plasmon is the collective oscillation of valence electrons at metal surfaces [21]. The coupling between surface plasmons and photons forms a quasi-particle called Surface Plasmon Polariton, which is an EM wave that travels along a metallic surface. SPPs in regular metals are always Transverse Magnetic (TM) electromagnetic waves since a Transverse Electric (TE) polarized EM field would have its electric component normal to the interface as a consequence it could not interact with the free electrons of the plasmonic materials [22].

Plasmonic materials are very exciting research field which has attracted the attention from multiple disciplines and has applied in a lot of applications because of their unique properties. Chemical and biological sensors have been developed by utilizing SPPs resonance as a sensitive function of the surrounding material [22]. In addition, SPPs have been also used in photon-scanning microscopy and imaging [22]. One of the most important features of plasmonic materials such as graphene is to enable THz band nanocommunication among nanosystems [4].

Groundbreaking experiments regarding two-dimensional (2D) materials have shown that graphene is an exceptional 2D plasmonic platform and it can be used as an alternative to noble metals [23]. Graphene is a one-atom-thick layer of carbon atoms arranged in a honeycomb 2D crystal lattice possessing unique electrical and optical properties, that is, graphene has the largest known electrical conductivity. Graphene has been proposed as a building material for plasmonic nanoantennas [4] and nanotransceivers [3]. Moreover, doped graphene has the ability to support propagation of tightly confined SPPs in the terahertz band (0.1–10 THz) at room temperature [16,24], enabling the miniaturization of nanotransceivers suited for wireless nanocommunication.

The excitation of SPPs can happen in several ways, which we will explain in Section 3.2. The generated SPPs are reasonably femtoseconds long pulses. Each technique requires energy to generate SPPs. The energy can be harvested using a suitable nanoscale energy harvester (see Section 3.1). The principle idea of generating SPPs is that we need to be on the resonance frequency and wavenumber in order to have the excitation. The resonance frequency at which SPPs are excited depends on the material conductivity. For instance, noble metals such as gold or silver support SPP waves in visible frequencies [25,26]. Unlike, noble metals, graphene supports SPPs at frequencies in the THz band (0.1–10 THz). By allowing wave propagation at the THz band (0.1–10 THz), the SPP waves can be generated with less power which might be feasible for nodes operated by nanoscale energy harvesters. The terahertz wave then propagates towards the antenna and is finally radiated [27].

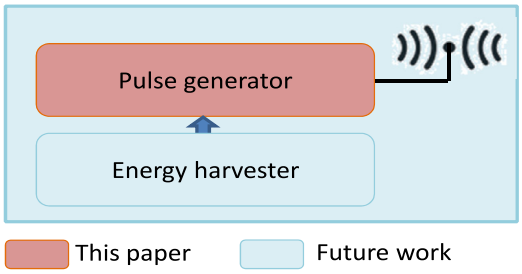

Fig. 1. Illustration of sensorless event detection node which includes an energy harvester and a pulse generator. A radio radiates the pulse in free space.

Recent studies confirm that SPPs provide a dominant contribution to the antenna radiation [20,28]. However, SPPs experience damping and, in turn, low resonance which can eventually affect the antenna radiation. We suggest how to improve the SPP resonance using our proposed pulse generator in Section 5. In the next section, we present a sensorless event detection node which consists of two components that an energy harvester and a pulse generator module. We also discuss the state of the art configurations for these two components.

3. Sensorless event detection node

A pulse-based events monitoring system is built from a sensorless event detection node and a base station. The sensorless node harvests energy from the event and transmits a pulse of proportional amplitude to a base station. The base station remotely detects the events based on the received energy observation [15]. However, this paper only focuses on the sensorless event detection node. An event detection node is composed of energy harvesting and a pulse generating system, respectively. In this section, we provide the theoretical analysis of different approaches for energy harvesting system and pulse generator.

It has been shown in the literature that there are many biological and chemical events of interest that dissipate energy when they take place [15]. The energy harvested from different events not only be used to power limited number of components but also to detect events at the same time. For example, in biomedical application, a blood flow [29], cardiac motions [30], lung and diaphragm motions [31] are all driving events which can be monitored directly from the harvested energy from these events. Similarly, the events "indoor" or "outdoor" can be monitored by analyzing the harvested energy because such energy would be larger when outdoor compared to indoor. In chemical reactions, different events take place at the catalytic site which produces a different amount of heat energy. Such energy can be converted into electricity [15]. If different events generate different amounts of energy, then conceptually, it is possible to use the harvested energy as a signature for event detection without employing any onboard sensors. The schematic diagram of sensorless event detection node is shown in Fig. 1 which has an energy harvester and a pulse generator. It is based on the idea that when an event occurs, the energy emitted by the event is harvested using a suitable nanoscale energy harvester (see Section 3.1). This harvested energy can be used to drive the pulse generator to produce a pulse whose energy is equal to the amount of harvested energy.

A pulse generator, which we will explain later in this section, is the element that takes electrical energy (DC) and generates femtoseconds long pulses [10]. A radio is an element which takes the pulse and radiates it. A proper rectification may be required if generated voltage is AC. In the following sections, we detail these two components of sensorless event detection node followed by theoretical analysis. In Section 4, we present our simple architecture for the pulse generator to generate THz pulses using near-field excitation.

3.1. Energy harvester

In recent years, researchers have developed different techniques for nanosystems to harvest energy from the events in the ambient environment using specialized nanomaterials. The discovery of these nanomaterials has greatly accelerated the development of nanosystems and to scavenge energy at nanoscale [32]. These techniques are as follows:

3.1.1. Piezoelectric

Piezoelectricity, also called the piezoelectric effect, is the appearance of an electrical potential across the sides of certain materials when they are subjected to mechanical stress. At the nanoscale, it is called nano-piezoelectricity. The discovery of piezoelectric nanomaterials provides a new opportunity to develop nanoscale energy harvesters called piezoelectric nanogenerators [33]. The nature of piezoelectricity comes from the non-centrosymmetricity in the crystal [32]. There are 32 crystal classes and 20 of them exhibit the piezoelectric effect. These materials include Lead zirconate titanate (*PZT*), barium titanate ($BaTiO_3$), zinc oxide (ZnO), gallium nitride (GaN), zinc sulfide (ZnS) and many more [32]. The authors in [34] show that using piezoelectric zinc oxide nanowire (NW) arrays, nanoscale mechanical energy can be converted into electricity. In particular, they find that a single zinc oxide of diameter 20 nm with the length of 200 nm can produce power up to 0.5 pW at one cycle of resonance [34]. Similarly, vertically align zinc oxide nanowire can generate 1.1 pW/μm^3 [35].

3.1.2. Thermoelectric

In this method, the temperature gradient is converted into electricity using Seebeck's effect. The Seebeck effect, named after the Baltic German physicist Thomas Johann Seebeck, is the conversion of heat flow into electricity at the junction of two dissimilar electrical conductors [36]. This type of energy harvesting is feasible for portable and pervasive computing devices, and in environments where thermal gradients exist [37]. In particular, human body heat can be converted into electricity using the temperature gradient between the body temperature and the outer medium. However, low gradient and limited heat transfer can affect the output power efficiency [36].

3.1.3. Triboelectric

The triboelectric also known as the triboelectric effect is a type of contact electrification in which certain materials become electrically charged. This is due to electrostatic induction after they come into frictional contact with a different material. Rubbing glass with fur, or a plastic comb through the hair can produce triboelectricity. Any materials which exhibit the triboelectrification effect, from metal, to polymer, and to silk can be candidates for fabricating triboelectric nanogenerators (TENGs). However, the ability of a material for gaining/losing electron depends on its polarity. For instance, the organic and inorganic films that exhibit opposite tribopolarity are used to generate the triboelectricity [38]. TANGs can be used to harvest vibration energy [39], and to convert magnetic force variation to electricity [40]. It is further observed in [41] that using TANG, a power density of 2.04 mW/cm^3 equivalent to 2 fW/μm^3 can be achieved by using micro/nano dual-scale polydimethylsiloxane (PDMS).

3.1.4. Pyroelectric

A pyroelectric nanogenerator is an energy harvesting device which converts the time-dependent temperature fluctuation into electricity by using nano-structured pyroelectric materials. Unlike thermoelectric, pyroelectric materials do not need a spatial gradient but they require temporal temperature changes [36,42]. Likewise, a pyroelectric nanogenerator made from a single nanowire

of zirconate titanate can be is used as a temperature sensor for detecting the change in temperature [43]. Using $BaTiO_3$ film of 200 nm thick in pyroelectric nanogenerator, output power of 3 pW/um^3 can be generated [44]. In pyroelectric nanogenerator, the amount of harvested power is proportional to the rate of temperature change, which makes it directly useful for nanoscale systems [37]. This means that pyroelectric nanogenerator can be used to power nanoscale devices in different applications where the temporal temperature fluctuation exists. For example, pyroelectric nanogenerator can be used to power nanosensor nodes deployed in catalyst sites within chemical reactors [15].

Theoretical analysis

So far, we discussed different types of nanoscale energy harvesters which can be used to generate energy from the embedded environment. The choice of the most suitable energy harvester depends on the application where the nanoscale energy harvesting node is deployed. The envisaged applications are biomedical, plant monitoring and chemical reactions where such energy harvesters can be used to harvest energy at the nanoscale. For example, in biomedical application, assuming a blood flow scenario, an estimated power of 1.28 pW can be generated by piezoelectric nanogenerator when ZnO nanowires bend by, for instance, a flow movement [29]. The generated power depends on the blood pressure and the frequency of the heart rate (pulse). Other sources such as heat energy might be a suitable choice to power a nanoscale energy harvesting node. For instance, in chemical reactions, different reactions (events) take place at the catalytic site which produces heat. The production of heat would increase the temperature of the site. This temperature gradient can be converted into electricity using pyroelectric nanogenerator [15]. However, if each reaction last for 1 ps then pyroelectric nanogenerator can harvest power within the range of few pico Watt (pW) [15]. If different events generate different amounts of energy, then the harvested energy can be used as a signature for event detection without employing an onboard sensor.

3.2. Pulse generator

The key component of the event monitoring node is the pulse generator. There are other configurations which are used to generate SPPs on the metallic and graphene surface. These SPPs lead to very short pulses, just several tens of femtoseconds long. Therefore, in what follows, we provide detail literature of configurations that are used to generate SPPs as shown in Fig. 2. At the end of this section, we will provide a discussion to elaborate the need for designing a simple model to generate THz pulses suitable for Tiny IoNT nodes.

3.2.1. Kretschmann–Raether configuration

The Kretschmann–Raether method is an Attenuated Total Reflection (ATR) method, where Total Internal Reflection (TIR) takes place [45]. In this method, a metallic film is sandwiched between a dielectric, usually a prism, and the air [45]. Light is incident from the dielectric side and SPPs are excited on the metal–air interface as shown in Fig. 3a). The parallel to interface component of incident light momenta (k_x) couples to the SPP wave number (k_{sp}) giving rise to SPP that which propagates along the interface (x direction) as it is shown by Fig. 3a). A restriction that Kretschmann–Raether method imposes is that it can be applied only for very thin metallic films up to 70 nm.

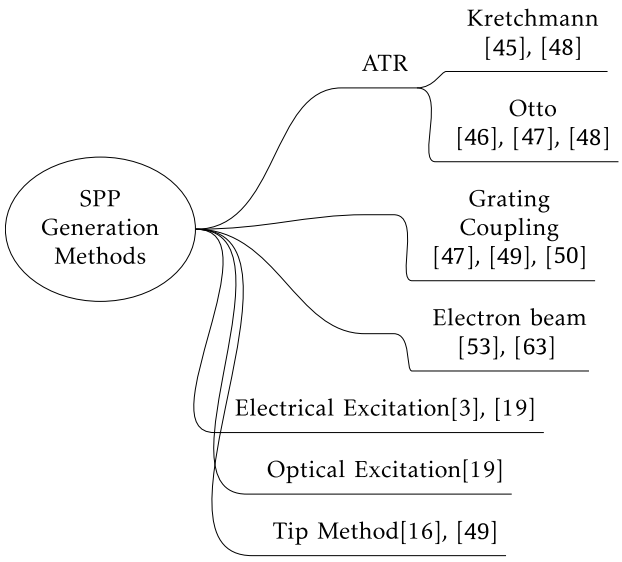

Fig. 2. Generating SPPs using different excitation methods.

3.2.2. Otto configuration

Otto method is similar with Kretschmann–Raether configuration but it follows different setting of metal and dielectrics, that is, an air gap is located between a metal and a dielectric (prism) [46,47]. The incidence light is projected from the prism side and SPP wave is excited on the air–metal interface [48] as shown in Fig. 3b). Likewise, in Kretschmann–Raether method, the parallel to interface component of the momentum of light must couple with the momentum of surface plasmon on the air–metal interface. Due to subwavelength character of SPP [49], the wave number k_x of incident EM wave is smaller than that of SPP wave k_{sp}, that is, a denser medium is used to bring the coupling condition between the light and SPP wave number, since the k_x takes higher values in dielectric than in light as Eq. (2) states. The coupling condition for surface plasmon waves in the metallic film [49] is given by

$$k_x = k_{sp}, \tag{1}$$

where the parallel to interface wave number component of incident light is

$$k_x = k_0\sqrt{\varepsilon_d}\sin(\theta_i) \tag{2}$$

and the SPP wave number is given by [47,50]

$$k_{sp} = k_0\sqrt{\frac{\varepsilon_m\varepsilon_d}{\varepsilon_m+\varepsilon_d}} \tag{3}$$

where $k_0 = \omega/c$ is the wave number in free space, ω is the operation angular frequency, c is the light velocity in vacuum, θ_i is the incidence angle of light wave and ε_d, ε_m are the dielectric permittivity for dielectric and for metallic film, respectively. The SPP dispersion relation is given by Eq. (3) at a metal–dielectric interface [49] where the metal permittivity is frequency dependent ($\varepsilon_m(\omega)$).

The Otto method as well as the Kretschmann–Raether, work on ATR configuration where TIR happens on the dielectric interface. That is, the EM wave comes from a denser medium with an angle greater than critical angle [51]. The SPP resonance is sharp and sensitive to the coupling condition and incidence angle. This method is useful when direct contact with the metal surface is undesirable, for instance when sensing molecular absorption of the surface is required.

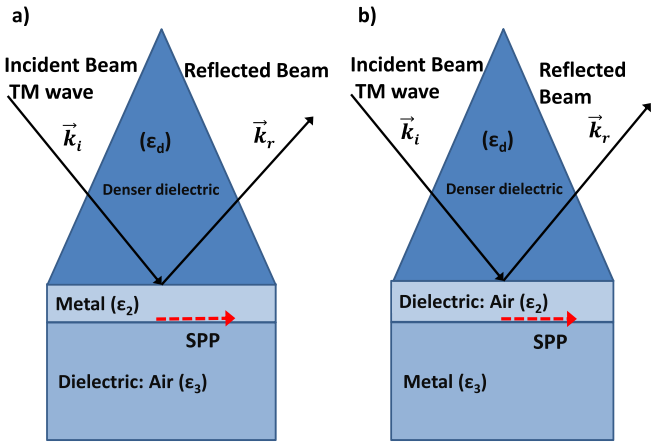

Fig. 3. Schematic representation of Attenuated Total Reflection (ATR) methods which are used for SPP excitation: (a) Kretschmann–Raether and (b) Otto Configuration.

3.2.3. SPP excitation by grating coupler

A grating coupler is formed by periodic slits or grooves on a metallic surface with lattice constant (grating period) a [47,49]. In a grating coupler, the momentum of incidence EM wave is coupled with the wave numbers of SPP (k_{sp}) resulting to SPP excitation [47, 50]. The wavenumber k_d of the incident light, which is always smaller than k_{sp}, is being increased by an amount proportional to the reciprocal wavenumber of grating $k_g = 2\pi/a$, until the satisfaction of the coupling condition

$$k_{sp} = k_d \sin\theta_i \pm k_g \nu, \tag{4}$$

where $k_d = k_0\sqrt{\varepsilon_d}$ the wavenumber of the incident light in a dielectric environment with permittivity ε_d, and ν is an integer.

The Eq. (4) states that when an incidence wave hits a grating surface, then the in-plane wave number ($k_d \sin\theta_i$) receives an additional momentum of $\pm k_g \nu$ leading to grating coupling. To achieve a successful grating coupling and SPP excitation, we have to tune correctly the parameters of the system, namely θ_i, a and ε_d. This method limits the dispersion distribution of the excited SPPs to a very narrow frequency range [52] as well as it requires very sensitive tuning and geometry restriction for meeting the coupling condition.

3.2.4. SPP excitation by electron beam

Exciting SPPs using electron beam is a different method than using EM radiation. In this method, a beam of electron propagates parallel to a metallic sheet. The phase velocity of the SPP wave must couple with that of the electron beam. It is further investigated in [53] that this condition holds only when periodic dielectric slits are introduced in a substrate and eventually the evanescent wave of the electron beam couples to SPPs. This method requires a continuous electron beam with tunable energy and periodic slits with the proper period.

3.2.5. Optical excitation

As it has already been mentioned, graphene provides the opportunity to enable communication at the nanoscale in the terahertz band [3,4,54].

In optical excitation method, graphene plasmonic antenna is fed with a photoconductive source, which is excited on its turn by an optical laser operated in the pulsed mode as reported in [18]. This way, SPPs are excited in the THz band when an external EM source with femtosecond pulse excites SPP on the interface between graphene sheet and dielectric [19]. The main intuitive in this method is when a biased semiconductor is excited by a laser pulse with photon energy greater than its bandgap then the SPP waves are generated at the interface between the graphene layer and the dielectric material.

3.2.6. Electrical excitation

In the electrical excitation mechanism, an induced electric voltage (DC) is applied between the source and the drain of a HEMT. Using this process, a plasma wave is generated, through the Dyakonov–Shur instability, which, in turn, is used to excite a propagating SPP wave at the interface with the graphene layer [19]. In this configuration, SPP wave is generated indirectly by first exciting 2D plasmons in the HEMT channel which in turn couples with plasmons in the graphene surface to generate SPP wave.

3.2.7. Tip method

The tip is a near-field excitation method which uses a nano-prob to excite SPP on the graphene surface. In this method, a short tip act as a point source with dimension $d \approxeq 25$ nm is illuminated using infrared beam [16]. Due to the small aperture size of the tip, the EM radiation ensuing from the tip with very high wavenumbers k. Hence, the matching condition between k and k_{sp} is naturally satisfied, and subsequently, SPP waves are excited [49]. Near-field excitation method is easy, robust and used for local excitation of SPPs in several plasmonic systems [16,17,49,55].

Theoretical analysis

We discussed different configurations for SPP excitation. The choice of the most suitable method depends on the operating frequency, the type of source, the metal permittivity, and the system configuration. However, integrating any of such configurations in event detection node at nanoscale further imposes size, complexity, computational and power limitations.

In visible regime, noble metals are used whereas in THz graphene shows plasmon resonance. For instance, silver and gold films are used in a Kretschmann–Raether configuration for photoemission effect [56], SPP imaging for bio-molecular interaction analysis [50], for testifying of blood cell analysis, serology analysis, and immunology [57]. On the other hand, Otto configuration is a suitable method in infrared range because of the thickness d of the gap between the denser dielectric and metal, increases accordingly to incidence wavelength [57]. Furthermore, the finite film thickness in Otto or Kretschmann configurations induces losses which reduces SPP intensity and propagation [58]. The grating coupler method is suitable for restricting the dispersion distribution of excited SPP to a very narrow frequency window [52]. This method further requires a special structure on the dielectric interface which may be difficult to produce. These studies do not provide solutions to generate SPPs in graphene in the THz band (0.1–10 THz). To excite SPPs in the THz band, HEMT circuit is introduced with a graphene-based gate in [3]. However, our work is different from these studies. The focus of our work is to investigate a novel concept for pulse generator which should be simple and can directly excite SPP on graphene surface in the THz band without the need to fabricate specialized circuits on the graphene surface. Using COMSOL Multiphysics, we will show that this method can generate SPPs in the THz band without employing any extra circuits which are usually required in existing methods.

4. The proposed pulse generator with near field excitation in THz band

This section presents the proposed pulse generator of a sensorless event detection node, as shown in Fig. 1. However, note that the methodology is general and can be generalized to any sensor node monitoring human lung cells [1,59], chemical reactions [60, 61] and so on. Assuming the δ amount of energy is harvested by

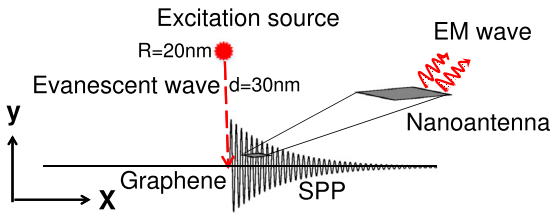

Fig. 4. Illustration of a pulse generator where SPP is excited on monolayer graphene sheet using the near-field method. A nanoantenna takes the SPP wave and radiates it into a free-space EM wave.

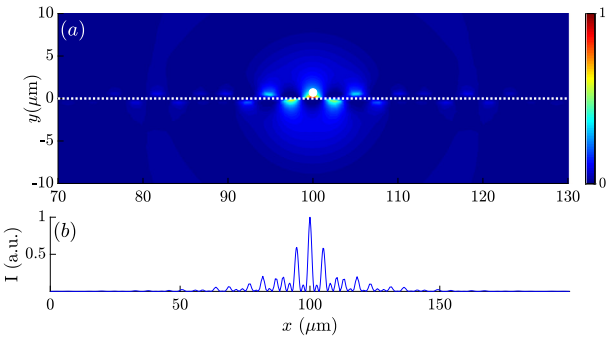

Fig. 5. The magnetic intensity I demonstrates the plasmon resonance on a doped graphene monolayer (dotted white line). The spatial distribution of I is represented in arbitrary values (a.u.) by (a) colorbar in x–y plane and by (b) with a solid blue line along the graphene layer ($y = 0$). An evanescent TM EM dipole source (n=1) of frequency $f = 10$ THz and with phase angle $\theta = \pi/2$ is located at $X_s = 100$ μm and $Y_s = 30$ nm above the graphene layer, indicated by a tiny white spot. The chemical potential of graphene is considered $\mu_c = 0.5$ eV. The SPP wavelength is calculated to be $\lambda_{sp} = 5$ μm.

the energy harvester from an event in the immediate environment. This energy can be used to drive the pulse generator to generate a THz pulse (see Fig. 1). If different events generate different amounts of energy, then conceptually, it is possible to use the harvested energy as a signature for event detection. However, due to the severe size restrictions and low complexity of the nanoscale device, the pulse generator must be kept simple which can directly generate the pulse in the terahertz band (THz). This is due to the fact that simple structures are more robust in the future design of nanodevices.

In this numerical study, we now investigate the pulse generator, to generate SPPs on the graphene surface using COMSOL Multiphysics. The schematic model of the proposed pulse generator is shown in Fig. 4. The pulse generator generates the SPP, which then propagates towards the plasmonic antenna. A plasmonic antenna converts SPP into propagating electromagnetic (EM) wave and finally radiates into the free space. The antenna modeling is beyond the scope of this paper. As it has been discussed previously, we use near-field excitation method to generate SPPs in the THz band which is simple and can produce Electromagnetic (EM) radiation with a wide range of high wavenumber. Hence, the coupling condition can be easily satisfied and consequently, the SPP wave can be excited which we will show in the next section.

In our modeling, we consider a surface conductivity model for infinitely large graphene sheets. Since graphene is a real 2D material, it is introduced as a boundary between two interfaces, namely as a surface current given by the Ohm law $\vec{J} = \sigma_g \vec{E}$, where σ_g is the complex optical conductivity of graphene [17]. In low frequencies, i.e. THz, σ_g is dominated by intraband transitions and can be approximated very well by the Drude model as [62]:

$$\sigma_g(\omega) = \frac{je^2\mu_c}{\pi\hbar^2(\omega + j\tau^{-1})}, \tag{5}$$

where e is the electron charge, $\hbar$ is the reduced Planck constant, ω is the angular frequency, τ is the scattering rate equal to $\tau = 0.5$ ps and μ_c is the chemical potential of graphene [17,62].

In what follows we consider a free standing graphene sheet, viz. graphene is surrounded by air with permittivity $\varepsilon_{air} = 1$. As a part of a future work, we will also evaluate the proposed model for finite size graphene sheet on dielectric material. Nevertheless, methodology in this paper is entirely general. For exciting SPPs, we use the near field method. In particular, very close to the graphene sheet we put a TM evanescent EM source, $\vec{E}$, with electric field components given by

$$\begin{pmatrix} E_x \\ E_y \\ E_z \end{pmatrix} = \begin{pmatrix} \cos(n(\phi - \theta)) \\ \sin(n(\phi - \theta)) \\ 0 \end{pmatrix} \tag{6}$$

where n is an integer and defines the evanescent character of source, viz. $n = 1$ corresponds to a dipole source, $n = 2$ to quadrupole and so on; θ is a constant phase and ϕ is a spatial depended phase defined as $\phi = \arctan 2(y - y_s, x - x_s)$ where (x_s, y_s) are the Cartesian coordinates of the source center and arctan 2() is the inverse function of the tangent function with two arguments. Using the near-field excitation method, we aim to explore the dependence of the plasmon resonance on the frequency f, on the doping amount μ_c of graphene, on the source phase θ and evanescent parameter n.

5. Results and discussion

In this section, we present numerical results of exciting SPPs using proposed pulse generator. The numerical simulations have been performed by the virtue of COMSOL for a 2D space. The graphene is considered as a surface boundary condition with conductivity given by Eq. (5) and extended along to the x axis [17]. The length of graphene, along with the x-direction, is chosen to be large enough (200 μm) to be considered as an infinite plane rather than a graphene nanoribbon. A circle of radius $R = 20$ nm has been located 30 nm above the graphene sheet. On the boundaries of the circle, we apply a TM electric field according to the Eq. (6), which is acting as a TM polarized excitation source since $R \ll \lambda$ (in the THz regime). Furthermore, perfect match layer (PML) boundary conditions have been imposed on all the edges.

5.1. The impact of frequency on the amplitude of SPP

In Fig. 5, we, first, present COMSOL result at $f = 10$ THz, $\mu_c = 0.5$ eV and for $\theta = \pi/2$. The magnetic field intensity I, associated with the only non-zero component of magnetic field $I = |H_z|^2$, is represented with color in Fig. 5(a) and with solid line in Fig. 5(b), normalized to maximum value of intensity. Plasmon resonance and propagating SPP waves are observed. The plasmon wavelength is calculated to be $\lambda_{sp} = 5$ μm, which is six times smaller than the light wavelength revealing the sub-wavelength character of the graphene plasmons.

We now proceed by investigating the plasmon resonance (amplitude) for several values of frequency in the THz regime, by keeping constant the rest parameters as in Fig. 5. The intensity I is a good metric to measure plasmon resonance, that is, a higher EM amplitude denotes a better plasmon resonance. Fig. 6 indicates the amplitude of I, normalized to its maximum value, as a function of frequency. We observed that a better plasmon resonance is achieved in higher frequencies of the THz band.

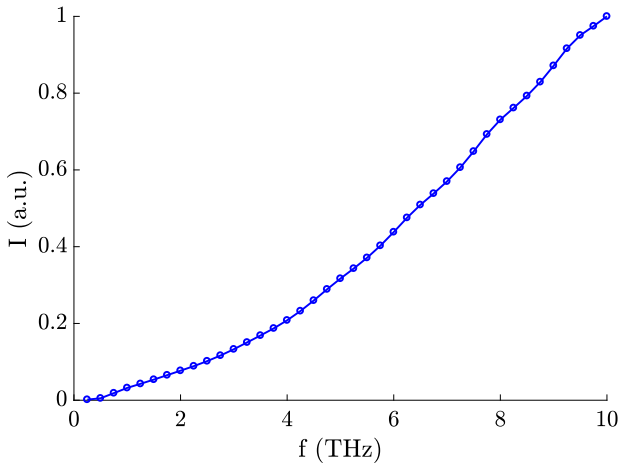

Fig. 6. The maximum value of I for several values of frequency is presented revealing that the higher the frequency the better plasmon resonance is achieved.

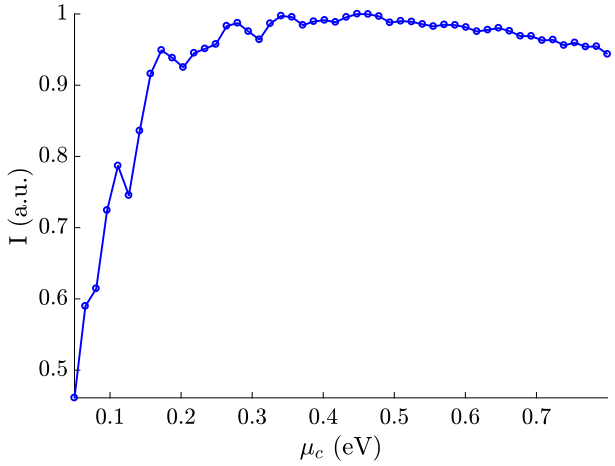

Fig. 7. The maximum value of I for several values of doping μ_c is shown revealing that at a certain frequency of $f = 10$ THz, the plasmon resonance is a increasing function of the doping for values $\mu_c < 0.4$ eV.

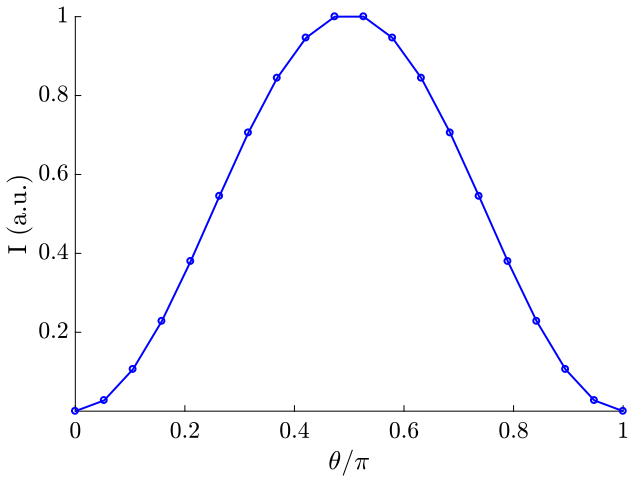

Fig. 8. The maximum value of I for several as function as the phase angle θ of the source is demonstrated with blue solid line. The best plasmon resonance is observed for the $\theta = \pi/2$.

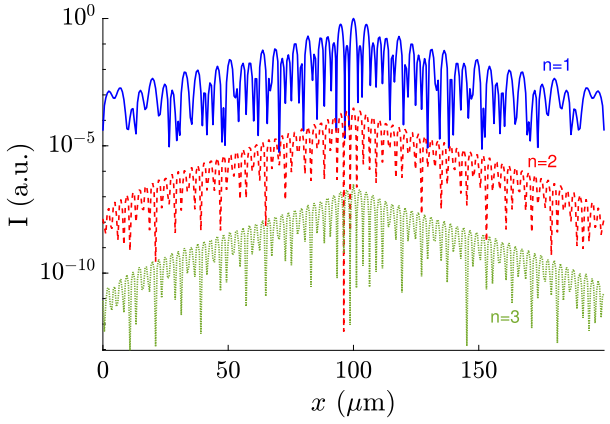

Fig. 9. The plasmon profile intensity I along the graphene sheet is represented for several values of evanescent parameter n of the source, that is, for $n = 1$, $n = 2$ and $n = 3$.

5.2. The impact of chemical potential on SPP resonance

Furthermore, we numerically investigate how the plasmon resonance depends on graphene doping at a certain frequency of $f = 10$ THz and for an evanescent source with $n = 1$ and $\theta = \pi/2$. In Fig. 7, we present the maximum amplitude of the intensity I for a range of chemical potential. We observe from Fig. 7 that the plasmon resonance is an increasing function of μ_c when it is less than 0.4 eV. In addition, we observe an abnormal behavior for values $\mu_c < 0.4$ eV. For larger values of $\mu_c > 0.43$ eV, the plasmon resonance is decreasing monotonically with μ_c.

5.3. The impact of phase angle of the evanescent source on the SPP resonance

The dependence of plasmon resonance on the source phase angle θ is displayed in Fig. 8. We observe that the plasmon intensity I follows a normal distribution, with respect to θ, with the best plasmon resonance achieved at $\theta = \pi/2$. This result indicates the strong dependence of the phase angle of the excitation source on the amplitude of the SPPs. Subsequently, when we use evanescent sources for excitation of SPPs, we have to take into account the optimization phase angle.

5.4. The impact of the type of evanescent source on the SPP resonance

Finally, by studying how the evanescent parameter n affects the plasmon resonance, we find that as the excitation source becomes more evanescent ($n > 1$) the plasmon resonance decrease dramatically. In Fig. 9 we present the profile I along the graphene layer for several values of the evanescent parameter. We observe that the plasmon resonance decreases dramatically as n increases. This is because of the quality of the plasmon excitation is inverse proportional to the evanescent parameter of the source (n), thus as larger is the n as faster the SPP amplitude drops.

6. Conclusion and future works

In this work, we proposed a new design of sensorless event detection node composed of the energy harvester, pulse generator, and a radio. We discussed the state of the art configurations for the energy harvesting and the THz pulse generation. We investigated the pulse generator within the sensorless event detection node and found that using the proposed method, THz pulses can be excited directly on the graphene surface without any prism, periodic slits

and special circuit. Simulations have been performed using COMSOL Multi-physics, which is a commercial Maxwell's equations solver in the frequency domain. The near-field method excites SPPs locally, which requires improvement in practice. Thus we explored how operating frequency, the doping amount of graphene and the properties of the evanescent source affect the plasmon resonance of SPPs. We found that plasmon resonance strongly depends on frequency, on doping amount and on the characteristics of an evanescent point source. In particular, we found that the higher the frequency, the better the achieved plasmon resonance. In addition, an EM dipole source ($n = 1$) with phase angle $\theta = \pi/2$ leads to the best observed plasmon resonance. We conclude that the proposed pulse generator scheme can be employed in designing of sensorless event detection node. As part of our future work, we will model energy harvesting component in COMSOL Multiphysics and will integrate it with the proposed pulse generator for the realization of operational sensorless event detection node.

Acknowledgments

The authors would like to thanks Prof. Chun Tung Chou for insightful discussions. M.M. acknowledges support by an EFRI 2-DARE NSF, United States Grant No. 1542807 and the ARO MURI Award, United States No. W911NF14-0247. We used computational resources on the Odyssey cluster of the FAS Research Computing Group at Harvard University.

References

[1] E. Zarepour, N. Hassan, M. Hassan, C.C. Tung, M.E. Warkiani, Design and Analysis of a Wireless Nanosensor Network for Monitoring Human Lung Cells, 2015.
[2] J.M. Jornet, I.F. Akyildiz, Channel modeling and capacity analysis for electromagnetic wireless nanonetworks in the terahertz band, IEEE Trans. Wireless Commun. 10 (10) (2011) 3211–3221.
[3] J.M. Jornet, I.F. Akyildiz, Graphene-based plasmonic nano-transceiver for terahertz band communication, in: Antennas and Propagation (EuCAP), 2014 8th European Conference on, IEEE, 2014, pp. 492–496.
[4] J.M. Jornet, I.F. Akyildiz, Graphene-based plasmonic nano-antenna for terahertz band communication in nanonetworks, IEEE J. Sel. Areas Commun. 31 (12) (2013) 685–694.
[5] I.F. Akyildiz, J.M. Jornet, The internet of nano-things, IEEE Wireless Commun. 17 (6) (2010) 58–63.
[6] S.J. Lee, C. Jung, K. Choi, S. Kim, Design of wireless nanosensor networks for intrabody application, Int. J. Distrib. Sens. Netw. 11 (7) (2015) 176761.
[7] A. Afsharinejad, A. Davy, B. Jennings, C. Brennan, Performance analysis of plant monitoring nanosensor networks at thz frequencies, IEEE Internet Things J. 3 (1) (2016) 59–69.
[8] E. Zarepour, M. Hassan, C.T. Chou, A.A. Adesina, Remote detection of chemical reactions using nanoscale terahertz communication powered by pyroelectric energy harvesting, in: Proceedings of the Second Annual International Conference on Nanoscale Computing and Communication, ACM, 2015, p. 8.
[9] J.M. Jornet, I.F. Akyildiz, Joint energy harvesting and communication analysis for perpetual wireless nanosensor networks in the terahertz band, IEEE Trans. Nanotech. 11 (3) (2012) 570–580.
[10] J.M. Jornet, I.F. Akyildiz, Femtosecond-long pulse-based modulation for terahertz band communication in nanonetworks, IEEE Trans. Commun. 62 (5) (2014) 1742–1754.
[11] K. Chi, Y.-h. Zhu, X. Jiang, V.C. Leung, Energy-efficient prefix-free codes for wireless nano-sensor networks using ook modulation, IEEE Trans. Wireless Commun. 13 (5) (2014) 2670–2682.
[12] K. Chi, Y.-h. Zhu, Y. Li, D. Zhang, V.C. Leung, Coding schemes to minimize energy consumption of communication links in wireless nanosensor networks, IEEE Internet Things J. 3 (4) (2016) 480–493.
[13] M. Pierobon, J.M. Jornet, N. Akkari, S. Almasri, I.F. Akyildiz, A routing framework for energy harvesting wireless nanosensor networks in the terahertz band, Wireless Netw. 20 (5) (2014) 1169–1183.
[14] Q.H. Abbasi, K. Yang, N. Chopra, J.M. Jornet, N.A. Abuali, K.A. Qaraqe, A. Alomainy, Nano-communication for biomedical applications: A review on the state-of-the-art from physical layers to novel networking concepts, IEEE Access 4 (2016) 3920–3935.
[15] E. Zarepour, M. Hassan, C.T. Chou, A.A. Adesina, Semon: Sensorless event monitoring in self-powered wireless nanosensor networks, ACM Transactions on Sensor Networks 13 (15).
[16] Z. Fei, A. Rodin, G. Andreev, W. Bao, A. McLeod, M. Wagner, L. Zhang, Z. Zhao, M. Thiemens, G. Dominguez, et al., Gate-tuning of graphene plasmons revealed by infrared nano-imaging, Nature 487 (7405) (2012) 82.
[17] M. Mattheakis, C.A. Valagiannopoulos, E. Kaxiras, Epsilon-near-zero behavior from plasmonic dirac point: Theory and realization using two-dimensional materials, Phys. Rev. B 94 (20) (2016) 201404.
[18] A. Cabellos-Aparicio, I. Llatser, E. Alarcon, A. Hsu, T. Palacios, Use of terahertz photoconductive sources to characterize tunable graphene rf plasmonic antennas, IEEE Trans. Nanotechnol. 14 (2) (2015) 390–396.
[19] J.M. Jornet, A. Cabellos, On the feeding mechanisms for graphene-based thz plasmonic nano-antennas, in: Nanotechnology (IEEE-NANO), 2015 IEEE 15th International Conference on, IEEE, 2015, pp. 168–171.
[20] H. Jia, H. Liu, Y. Zhong, Role of surface plasmon polaritons and other waves in the radiation of resonant optical dipole antennas, Sci. Rep. 5 (2015) 8456.
[21] J. Pitarke, V. Silkin, E. Chulkov, P. Echenique, Theory of surface plasmons and surface-plasmon polaritons, Rep. Prog. Phys. 70 (1) (2006) 1.
[22] D. Sarid, W. Challener, Modern introduction to surface plasmons: theory, Mathematica modeling, and applications, Cambridge University Press, 2010.
[23] A. Grigorenko, M. Polini, K. Novoselov, Graphene plasmonics, Nat. Photonics 6 (11) (2012) 749.
[24] L. Ju, B. Geng, J. Horng, C. Girit, M. Martin, Z. Hao, H.A. Bechtel, X. Liang, A. Zettl, Y.R. Shen, et al., Graphene plasmonics for tunable terahertz metamaterials, Nature Nanotechnol. 6 (10) (2011) 630–634.
[25] M. Nafari, J.M. Jornet, Metallic plasmonic nano-antenna for wireless optical communication in intra-body nanonetworks, in: Proceedings of the 10th EAI International Conference on Body Area Networks, ICST (Institute for Computer Sciences, Social-Informatics and Telecommunications Engineering, 2015, pp. 287–293.
[26] M.H. Rehmani, A.-S.K. Pathan, Emerging Communication Technologies Based on Wireless Sensor Networks: Current Research and Future Applications, CRC Press, 2016.
[27] E. Zarepour, M. Hassan, C.T. Chou, A.A. Adesina, Energy-harvesting nanosensor networks: Efficient event detection, IEEE Nanotechnol. Mag. 10 (4) (2016) 4–12.
[28] C. Liu, H. Liu, Y. Zhong, Impact of surface plasmon polaritons and other waves on the radiation of a dipole emitter close to a metallic nanowire antenna, Opt. Express 22 (21) (2014) 25539–25549.
[29] S. Canovas-Carrasco, A.-J. Garcia-Sanchez, F. Garcia-Sanchez, J. Garcia-Haro, Conceptual design of a nano-networking device, Sensors 16 (12) (2016) 2104.
[30] B. Lu, Y. Chen, D. Ou, H. Chen, L. Diao, W. Zhang, J. Zheng, W. Ma, L. Sun, X. Feng, Ultra-flexible piezoelectric devices integrated with heart to harvest the biomechanical energy, Sci. Rep. 5 (2015) 16065.
[31] C. Dagdeviren, B.D. Yang, Y. Su, P.L. Tran, P. Joe, E. Anderson, J. Xia, V. Doraiswamy, B. Dehdashti, X. Feng, et al., Conformal piezoelectric energy harvesting and storage from motions of the heart, lung, and diaphragm, Proc. Natl. Acad. Sci. 111 (5) (2014) 1927–1932.
[32] Z.L. Wang, Y. Liu, Piezoelectric Effect at Nanoscale, Springer Netherlands, Dordrecht, 2014, pp. 1–18, http://dx.doi.org/10.1007/978-94-007-6178-0_273-2.
[33] Z.L. Wang, Zno nanowire and nanobelt platform for nanotechnology, Mater. Sci. Eng. R 64 (3) (2009) 33–71.
[34] Z.L. Wang, J. Song, Piezoelectric nanogenerators based on zinc oxide nanowire arrays, Science 312 (5771) (2006) 242–246.
[35] G. Zhu, R. Yang, S. Wang, Z.L. Wang, Flexible high-output nanogenerator based on lateral zno nanowire array, Nano Lett. 10 (8) (2010) 3151–3155.
[36] G. Sebald, D. Guyomar, A. Agbossou, On thermoelectric and pyroelectric energy harvesting, Smart Mater. Struct. 18 (12) (2009) 125006.
[37] E. Zarepour, Efficient communication protocols for wireless nanoscale sensor networks (Ph.D thesis), University of New South Wales, Sydney, Australia, 2015.
[38] S. Wang, L. Lin, Z.L. Wang, Nanoscale triboelectric-effect-enabled energy conversion for sustainably powering portable electronics, Nano Lett. 12 (12) (2012) 6339–6346.
[39] W. Yang, J. Chen, G. Zhu, J. Yang, P. Bai, Y. Su, Q. Jing, X. Cao, Z.L. Wang, Harvesting energy from the natural vibration of human walking, ACS Nano 7 (12) (2013) 11317–11324.
[40] M. Han, X.-S. Zhang, X. Sun, B. Meng, W. Liu, H. Zhang, Magnetic-assisted triboelectric nanogenerators as self-powered visualized omnidirectional tilt sensing system, Sci. Rep. 4.
[41] M. Han, X.-S. Zhang, B. Meng, W. Liu, W. Tang, X. Sun, W. Wang, H. Zhang, r-shaped hybrid nanogenerator with enhanced piezoelectricity, ACS Nano 7 (10) (2013) 8554–8560.
[42] Y. Yang, W. Guo, K.C. Pradel, G. Zhu, Y. Zhou, Y. Zhang, Y. Hu, L. Lin, Z.L. Wang, Pyroelectric nanogenerators for harvesting thermoelectric energy, Nano Lett. 12 (6) (2012) 2833–2838.
[43] Y. Yang, Y. Zhou, J.M. Wu, Z.L. Wang, Single micro/nanowire pyroelectric nanogenerators as self-powered temperature sensors, ACS Nano 6 (9) (2012) 8456–8461.

[44] B. Bhatia, A.R. Damodaran, H. Cho, L.W. Martin, W.P. King, High-frequency thermal-electrical cycles for pyroelectric energy conversion, J. Appl. Phys. 116 (19) (2014) 194509.
[45] E. Kretschmann, H. Raether, Radiative decay of non radiative surface plasmons excited by light, Z. Naturforsch. A 23 (12) (1968) 2135–2136.
[46] A. Otto, Excitation of nonradiative surface plasma waves in silver by the method of frustrated total reflection, Z. Phys. A 216 (4) (1968) 398–410.
[47] H. Raether, Surface plasmons on gratings, in: Surface Plasmons on Smooth and Rough Surfaces and on Gratings, Springer, 1988, pp. 91–116.
[48] S. Yushanov, L. Gritter, J. Crompton, K. Koppenhoefer, Surface plasmon resonance, in: COMSOL Conference, 2012.
[49] S.A. Maier, Plasmonics: Fundamentals and Applications, Springer Science & Business Media, 2007.
[50] S. Löfås, M. Malmqvist, I. Rönnberg, E. Stenberg, B. Liedberg, I. Lundström, Bioanalysis with surface plasmon resonance, Sensors Actuators B 5 (1–4) (1991) 79–84.
[51] Y.V. Bludov, A. Ferreira, N. Peres, M. Vasilevskiy, A primer on surface plasmon-polaritons in graphene, Internat. J. Modern Phys. B 27 (10) (2013) 1341001.
[52] P. Karpinski, A. Miniewicz, Surface plasmon polariton excitation in metallic layer via surface relief gratings in photoactive polymer studied by the finite-difference time-domain method, Plasmonics 6 (3) (2011) 541–546.
[53] S. Liu, C. Zhang, M. Hu, X. Chen, P. Zhang, S. Gong, T. Zhao, R. Zhong, Coherent and tunable terahertz radiation from graphene surface plasmon polaritons excited by an electron beam, Appl. Phys. Lett. 104 (20) (2014) 201104.
[54] I.F. Akyildiz, J.M. Jornet, Electromagnetic wireless nanosensor networks, Nano Commun. Netw. 1 (1) (2010) 3–19.
[55] M. Mattheakis, T. Oikonomou, M.I. Molina, G.P. Tsironis, Phase transition in pt symmetric active plasmonic systems, IEEE J. Sel. Top. Quantum Electron. 22 (5) (2016) 76–81.
[56] C. Macek, A. Otto, W. Steinmann, Resonant photoemission from aluminium films at 5 ev photon energy due to nonradiative surface plasma waves, Phys. Status Solidi (b) 51 (1) (1972) K59–K61.
[57] D. Barchiesi, A. Otto, Excitations of surface plasmon polaritons by attenuated total reflection, revisited, Riv. Nuovo Cimento 36 (2013) 173–209.
[58] A. Drezet, A. Hohenau, D. Koller, A. Stepanov, H. Ditlbacher, B. Steinberger, F. Aussenegg, A. Leitner, J. Krenn, Leakage radiation microscopy of surface plasmon polaritons, Mater. Sci. Eng. B 149 (3) (2008) 220–229.
[59] E. Zarepour, M. Hassan, C.T. Chou, M.E. Warkiani, Characterizing terahertz channels for monitoring human lungs with wireless nanosensor networks, Nano Commun. Netw. 9 (2016) 43–57.
[60] E. Zarepour, M. Hassan, C.T. Chou, A.A. Adesina, Open-loop power adaptation in nanosensor networks for chemical reactors, IEEE Trans. Mol. Biol. Multi-Scale Commun. 1 (3) (2015) 292–307.
[61] E. Zarepour, M. Hassan, C.T. Chou, A.A. Adesina, M.E. Warkiani, Reliability analysis of time-varying wireless nanoscale sensor networks, in: Nanotechnology (IEEE-NANO), 2015 IEEE 15th International Conference on, IEEE, 2015, pp. 63–68.
[62] M. Mattheakis, G.P. Tsironis, E. Kaxiras, Graphene and active metamaterials: theoretical methods and physical properties, arXiv preprint arXiv:1704.01912.
[63] E.J.R. Vesseur, J. Aizpurua, T. Coenen, A. Reyes-Coronado, P.E. Batson, A. Polman, Plasmonic excitation and manipulation with an electron beam, MRS Bull. 37 (8) (2012) 752–760.

Najm Hassan received the Bachelor's degree in Comp. Science from the University of Peshawar, in 2002, the Master's degree in Information Technology from Gomal University, in 2006, and the MS degree in networking from National University of Sciences and Technology (NUST) Islamabad, Pakistan, in 2009. He is currently third year PhD student at School of Computer Science and Engineering (CSE), UNSW, Australia. He has worked in the IT industry for five years. From 2010 to 2013, he served as Assistant Head of IT technical support at Emirates College of Technology Abu Dhabi U.A.E. In 2014, he also worked as IT Lecturer in Shinas College of Technology Sultanate of Oman. His research interests include nanoscale communication in the THz band, specializing in designing efficient communication protocols for events and nodes detection in wireless nanoscale sensor networks.

Marios Mattheakis received the B.S., M.S., and Ph.D. degrees in Physics from the University of Crete, Greece, in 2010, 2012, and 2014, respectively. Currently, he is a postdoctoral fellow in Prof. in Prof. Kaxiras team in Harvard University. His current research interests include plasmonics in two-dimensional materials like graphene, EM wave propagation in random networks and plasmonic metamaterials. https://scholar.harvard.edu/marios_matthaiakis.

Ming Ding is a researcher at Data 61, Australia. He received his B.S. and M.S. degrees with first class honours in Electronics Engineering from Shanghai Jiao Tong University (SJTU), China, in 2004 and 2007, respectively. In Apr. 2007, he joined Sharp Laboratories of China (SLC) as a Researcher. From Sep. 2007 to Sep. 2011, he pursued his Doctor in Philosophy (Ph.D.) at SJTU the same time working as a Researcher/Senior Researcher at SLC. In Dec. 2011, he achieved his Ph.D. in Signal and Information Processing from SJTU and work for SLC as a Senior Researcher/Principal Researcher until Sep. 2014 when he joined National Information and Communications Technology Australia (NICTA). In Sep. 2015, Commonwealth Scientific and Industrial Research Organization (CSIRO) and NICTA joined forces to create Data 61, where he research in this new R&D center located in Australia. been working on B3G, 4G, and 5G wireless for more than 9 his research interests include synchronization, MIMO technology, cooperative communications, heterogeneous networks, device-to-device communications, and modelling of wireless communication systems. Besides, he served as the Algorithm Design Director and Programming Director for an of future telecommunication networks in SLC for more than 7 years. Up to now, Ming has published more than 30 papers in IEEE journals and conferences, all in recognized venues, and about 20 3GPP standardization contributions, as well as a Springer book "Multi-point Cooperative Communication Systems: Theory and Applications". Also, as the first inventor, he holds 8 CN, 2 JP, 2KR patents and filed another 30 patent applications on 4G/5G technologies. For his inventions and publications, he was the recipient of the President's Award of SLC in 2012 and served as one of the key members in the 4G/5G standardization team was awarded in 2014 as Sharp Company Best Team: LTE Standardization Patent Portfolio. Ming is or has been guest editor/co-chair/TPC member of several IEEE top-tier journals/conferences, e.g., IEEE JSAC, IEEE Comm. Mag., IEEE Globecom workshops.